Mechanisms of Water Exchange between Lanthanide(III) Aqua Ions $[Ln(H_2O)_n]^{3+}$ and Bulk Water: A Molecular Dynamics Simulation Approach Including High-Pressure Effects

Thomas Kowall, François Foglia, Lothar Helm and André E. Merbach*

Abstract: We studied the microscopic mechanisms of the water exchange reaction between the hydration shells of lanthanide(III) ions (Ln = Nd, Sm, Yb) and bulk water by means of molecular dynamics simulations. In contrast to the residence time of a water molecule in the first hydration shell (τ_{res} (1st shell) = 1577, 170 and 410 ps for Nd^{3+}, Sm^{3+} and Yb^{3+}, respectively), that in the second hydration shell is nearly independent of the type of the cation and amounts to 12–18 ps. Along the lanthanide series a change in the coordination number from 9 to 8 is coupled to a changeover in the water exchange mechanism. The observed water exchange events on the $[Nd(H_2O)_9]^{3+}$ aqua ion follow a dissociatively activated I_d mechanism via an eightfold-coordinated transition state of square antiprismatic geometry. The lifetime of the transitory square antiprism varies between virtually 0 and 10 ps. The assignment of an I_d mechanism (instead of a limiting D mechanism) is supported by the existence of a preferential arrangement between the exchanging water molecules (180°) and by the fact that the calculated average activation volume $\Delta V^{\neq} = +4.5\ cm^3\,mol^{-1}$ is clearly smaller than the estimated activation volume $\Delta V^{\neq}_{lim} \approx \Delta V^0 = +7.2\ cm^3\,mol^{-1}$ for a limiting D process. In the case of Sm^{3+} a ninth water molecule exchanges frequently between the first hydration shell and the bulk and maintains the coordination equilibrium between a $[Sm(H_2O)_8]^{3+}$ and a $[Sm(H_2O)_9]^{3+}$ aqua ion. The resulting trajectory pattern of incoming and leaving water molecules is an alternation of elimination and addition reactions and cannot be classified into the scheme of D, I or A mechanisms for substitution processes. The reaction volume ΔV^0 for the coordination equilibrium $[Sm(H_2O)_8]^{3+} + H_2O \rightleftharpoons [Sm(H_2O)_9]^{3+}$ can be evaluated consistently both by a thermodynamic and a geometric approach. The observed exchange events for $[Yb(H_2O)_8]^{3+}$ exhibit the characteristics of an I_a mechanism. The water exchange takes place via a transition-state geometry close to that of a tricapped trigonal prism and involves a slightly negative activation volume.

Keywords
computer simulations · high-pressure chemistry · lanthanide complexes · ligand exchange · mechanistic studies

Introduction

This article is part of an overall project to present the microscopic picture of the water exchange reaction around tripositive lanthanide ions Ln^{3+} in aqueous solution [Eq. (1)] as it emerges from classical molecular dynamics (MD) simulations. In a

$$[Ln(H_2O)_n]^{3+} + {}^*H_2O \longrightarrow [\neq] \longrightarrow [Ln(H_2O)_{n-1}{}^*H_2O]^{3+} + H_2O \quad (1)$$

a first attempt we used Monte Carlo simulations and empirical pair potentials to study both the hydration of Ln^{3+} ions and the mechanism of water exchange.[1] For all Ln^{3+} ions studied we found an equilibrium between appreciable amounts of an eight-coordinated and a nine-coordinated aqua ion and no well-defined integer coordination numbers. Moreover, estimated activation barriers for the exchange of coordinated water were considerably smaller than the experimental values. In a subsequent article[2] we presented an improved description of the Ln^{3+}–water interaction. Inclusion of a water polarization term specially adapted to the high positive charge of the cation and to the strong radial orientation of the water dipoles in the first hydration shell led to a much more balanced and better reproduction of experimental structural[3] and kinetic data[4] compared with a nonpolarizable model.[5]

Concerning the coordination of Ln^{3+} aqua ions, the following picture emerged from the simulations.[2] Ln^{3+} ions are capable of forming aqua ions of coordination number eight and nine. Along the lanthanide series with decreasing ionic radius the coordination equilibrium shifts from predominantly ninefold coordination for a light lanthanide (Nd^{3+}) to predominantly eightfold coordination for a heavy lanthanide (Yb^{3+}). In the middle of the series (Sm^{3+}) an equilibrium between comparable amounts of an octaaqua and a nonaaqua ion results in an increased water exchange rate, compared with those Ln^{3+} ions where the equilibrium is totally shifted to either the nona- or octaaqua ion.

In a more recent paper[6] we analysed the structure and the internal dynamics of the first hydration shell. Projecting the first

[*] Prof. A. E. Merbach, T. Kowall, F. Foglia, L. Helm
Institut de Chimie Minérale et Analytique
Université de Lausanne, Bâtiment de Chimie (BCH)
CH-1015 Lausanne (Switzerland)
Fax: Int. code +(21)692 3875

  0947-6539/96/0203-0285 $ 15.00+.25/0

hydration shell onto the geometry of a regular polyhedron proved to be a valuable tool for the investigation of the local angular structure of the first hydration shell and its internal rearrangement. An octaaqua ion adopts a square antiprismatic geometry, whereas the water molecules of a nonaaqua ion have a strong tendency to form a tricapped trigonal prism. Tracing the orientation of the main symmetry axis of the hydration polyhedron as a function of time revealed internal rearrangements of the first hydration shell as spontaneous 90° pseudorotations of the polyhedron in the case of both a square antiprism and a tricapped trigonal prism. The simulated lifetime of a square antiprism between two rearrangements was in accord with the experimentally known timescale of symmetry fluctuations of the first hydration shell of the $[Gd(H_2O)_8]^{3+}$ aqua ion. From our simulations we were able to provide a mechanistic description of these symmetry fluctuations.

Rates for the exchange of coordinated water were found to lie in the subnanosecond regime and are therefore within the reach of MD simulations carried out on today's workstations.[2] Based on the insight gained into the equilibrium properties of the lanthanide aqua ions, the present article will focus on the mechanisms of their water exchange reactions and on the nature of the intermediates [+] in [Eq. (1)].

Experimentally the water exchange rate for Ln^{3+} ions can be obtained from NMR kinetic measurements.[7] The microscopic nature of the underlying reaction mechanism, however, is only indirectly accessible to experimental methods. In general, reaction mechanisms are suggested from experimentally testing the sensitivity of the reaction rate to a variety of chemical and physical parameters.[8] For the water exchange around Ln^{3+} ions activation volumes $\Delta V^{\neq}$ can be accurately determined from variable-pressure NMR kinetic experiments.[4a] $\Delta V^{\neq}$, a macroscopic pseudothermodynamic quantity, is a measure of the degree of bond formation or bond breakage that occurs in the transformation to the transition state and constitutes a fundamental clue as to the microscopic nature of substitution reactions and to their mechanistic classification.[8] For a general substitution reaction three simple pathways can be conceived:[8, 9] a dissociative (D) process with an intermediate of reduced coordination number; an associative (A) process with an intermediate of increased coordination number; an interchange (I) process, with synchronous bond-making and bond-breaking and no intermediate of lower or higher coordination number. In aqueous solutions a $\Delta V^{\neq}$ of $-6\,cm^3\,mol^{-1}$ has been found for the heavy Ln^{3+} ions of coordination number eight (Tb^{3+} to Tm^{3+})[4a] and has been interpreted in terms of an associative interchange I_a mechanism, with bond formation being the primary step during the interchange of the water molecules. Unfortunately, experimental data from NMR kinetic measurements for the water exchange rates and for the activation volumes are still lacking for the lighter Ln^{3+} ions of coordination number 9, owing to their less favourable magnetic properties.

MD simulations, which are based on a reliable interaction potential function as the most crucial ingredient, provide an independent approach for studying the water exchange on Ln^{3+} ions directly on a microscopic scale. From a methodological point of view the hydration of Ln^{3+} ions constitutes an ideal problem for classical MD simulations, because the interaction between the Ln^{3+} ion and "hard" oxygen-donor ligands like water is nondirectional without covalent contributions, so that ion–water forces can be represented well by simple Coulomb and van der Waals terms.[10] At the same time a change of the water exchange rate and of the water exchange mechanism along the series of Ln^{3+} ions should be mainly caused by steric packing effects and nonbonding interactions in the first hydration shell, and not by differences in the electronic structure of the lanthanide cation. Eventually, the analysis of MD simulations should allow the interpretation of the experimental results for the heavy lanthanide ions (CN = 8) and to make predictions for the lighter lanthanides.

In Section 2 the residence times of a shell water molecule along the lanthanide series are compared for the first and second hydration shell. For a direct classification of the exchange mechanism, characteristic distance and angle trajectories for the exchanging water molecules are presented in Sections 3 and 4. In Section 5 we look directly at the geometry of the intermediates and transition states involved. The usefulness of a quantitative geometric definition of the volume of a lanthanide aqua ion is tested in Section 6. Full activation volume profiles for the water exchange reactions are then presented in Section 7.

Results and Discussion

1. Method of simulation: The change of properties along the series of Ln^{3+} ions was pursued by means of three molecular-dynamics simulation systems from our previous paper[2] that took into account the polarization of water molecules in the first hydration shell and were denoted as Nd, Sm and Yb. The simulated systems were taken as representative models for aqueous solutions of Nd^{3+}, Sm^{3+} and Yb^{3+} ions, and yielded coordination numbers (CN) of 9, 8.5 and 8, respectively. These simulations will be further analysed in this article in order to gain insight into the water exchange kinetics and the water exchange mechanisms.

For Yb^{3+} and Sm^{3+} the simulation time was 1048 ps for a system of 1 cation and 300 water molecules. Because only three water exchange events occured on a Nd^{3+} ion during a simulation time of 1048 ps, we prolonged this simulation to achieve better statistics and all results for Nd^{3+} presented in this article are based on a total simulation time of 3146 ps. Further technical details of the simulation procedure are given in ref. [2]. The procedure that assigned the regular polyhedron closest to the geometry of the first hydration shell (a square antiprism for CN = 8 and a tricapped trigonal prism for CN = 9) and was used in the following analysis was described in our last paper.[6]

2. Residence time of a water molecule in the first and the second hydration shell: The method by which exchange rates for water molecules in the first hydration shell were extracted from the simulations is described in ref. [2]. From simulations Sm and Yb we found 50 and 19 exchange events per nanosecond. From the prolonged simulation Nd, 15 exchange events occured within 3.146 ns (Fig. 1a), that is, 5 exchange events per nanosecond. The maximum in kinetic lability of the first hydration shell in the middle of the lanthanide series (Sm^{3+}) is in accord with experimental findings and is interpreted as follows.[2, 4b] Along the series of the lanthanide ions with decreasing ionic radius the nonaaqua complex becomes more labile, whereas the kinetic lability of the octaaqua complex decreases. The fact that for a Ln^{3+} ion in the middle of the series comparable amounts of eight- and ninefold-coordinated aqua ions are in coexistence then favours fast kinetics between the two. In continuation it will be interesting to check whether an analogous effect is still observable for the water exchange in the second hydration shell. From our simulations, the picture of a still-structured second hydration shell emerged.[6] Water dipoles in the second shell still exhibit a marked radial alignment. Furthermore, when going from the first to the second shell the coordination number ap-

0947-6539/96/0203-0286 $ 15.00+.25/0 Chem. Eur. J. 1996, 2, No. 3

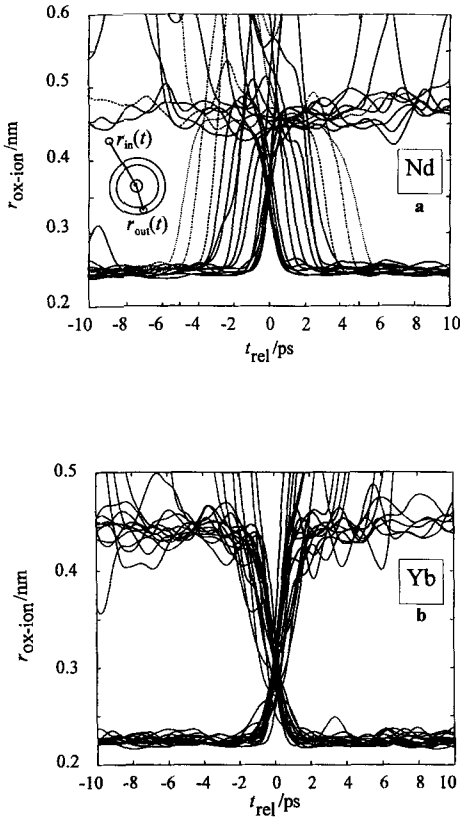

Fig. 1. a) Superposition of the trajectories for the fifteen exchange events observed for simulation Nd (CN = 9) in 3.146 ns after convolution with a Gauss function. b) As a) for the nineteen exchange events observed for simulation Yb (CN = 8) in 1.048 ns.

proximately doubles, with each water molecule of the first sphere binding two water molecules of the second sphere through linear hydrogen bonds.

Because the number of exchange events is considerably higher for the second than for the first hydration shell, simply counting the exchange events is no longer convenient and it is more appropriate to calculate directly the time correlation function $p(t)$ for the residence probability of a water molecule in a particular shell. $p(t)$ is the probability that after a time t a water molecule has never left its hydration shell; the mathematical definition can be found in ref. [11]. $p_{1st\ shell}(t)$ for the first hydration shell is displayed in Figure 2 (dashed lines), and the times of residence of a particular water molecule from an exponential fit (τ_{res} (1st shell) = 1577, 170 and 410 ps for simulations Nd, Sm and Yb, respectively) are consistent with the above-mentioned number of exchange events. For the definition of the second hydration shell we applied a geometric criterion that requires $3.7 < r_{ion-oxygen} < 5.4$ Å with reference to the pair distribution functions $g_{ion-oxygen}(r)$ in ref. [2]. The relevant time correlation functions in Figure 2 (solid lines) yielded residence times τ_{res} (2nd shell) of 13, 12 and 18 ps for simulations Nd, Sm and Yb. The slightly higher value for Yb^{3+} is certainly caused by its smaller ionic radius, but taking into account the fact that geometric definition is less clear-cut for the second shell than for the first shell, there is no longer a marked dependence of τ_{res} (2nd shell) on the type of the lanthanide ion. Apparently, the slight differences in the ionic radii are no longer perceptible in the second shells, and the behaviour of the second shells is dominated by the long-range Coulomb interaction with a point charge +3 and by the hydrogen bonding with the first shell water molecules. This contrasts with the marked dependence of the residence time in the first hydration shells on the type of the lanthanide ion that stems from the ability of Ln^{3+} aqua ions to form two discrete and geometrically well-defined species of coordination number eight and nine.

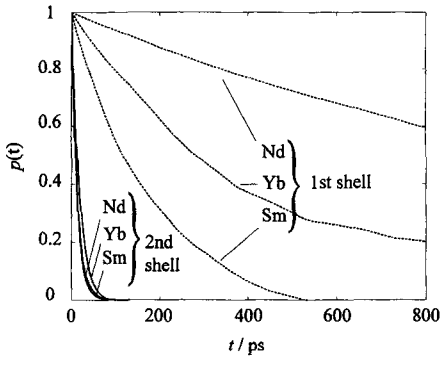

Fig. 2. Residence probability $p(t)$ that a shell water molecule still belongs to its hydration shell after a correlation time t, calculated for the simulations Nd, Sm and Yb (dashed lines: first shell; solid lines: second shell).

On the experimental side, kinetic exchange data for the second hydration shell of lanthanide ions were not available, but a comparison with the tripositive hexaaqua chromium complex $[Cr(H_2O)_6]^{3+}$ is instructive. Its six firmly bound water molecules in the first coordination sphere have a very long time of residence ($t_{res} \approx 20$ h[12]). The fact that the $[Cr(H_2O)_6]^{3+}$ unit is interacting with a second hydration shell of about 13 water molecules[13] suggests that, much as with the hydration of the lanthanide ions,[2] each water molecule of the first shell binds two water molecules in the second shell. Owing to the inertness of its first hydration shell and to its paramagnetism, the Cr^{3+} aqua ion is a favourable case in which a time of residence in the second hydration shell can be extracted from NMR measurements; a value of about 100 ps has been obtained.[14] The fact that the simulated residence times τ_{res} (2nd shell) for the lanthanide ions are one order of magnitude less than this value is in qualitative agreement with experimental findings from infrared spectroscopy that indeed confirmed a more structured and less labile second sphere in the case of Cr^{3+} compared with the lanthanide ions.[15]

3. Mechanistic classification of the water exchange in the first hydration sphere: In a basic approach all exchange events should be resolvable into pairs of mutually exchanging water molecules [cf. Eq. (1)]. The difference in time between the entry of a water molecule and the departure of a water molecule from the first hydration shell then allows the classification of the exchange process as an associative, dissociative or interchange mechanism. We identified from the simulations all transitions between the first hydration shell and the bulk and grouped them into pairs of water molecules that together form a coupled exchange. Subsequently, the exchange pathways of these pairs, that is, the ion–oxygen distance as a function of time, were convoluted with a Gauss function (σ = 0.4 ps) in order to suppress stochastic detail (see ref. [2]) and were then superimposed with respect to a common origin in time. The origin is the average between the two times when the leaving and the incoming water molecules crossed the boundary between the first and the second hydration shell.

The result for simulation Nd is shown in Figure 1a. The 15 exchange events that took place on the $[Nd(H_2O)_9]^{3+}$ aqua ion during the simulation time of 3.1 ns are of dissociative character throughout and the assignment of a dissociative interchange I_d mechanism seems most adequate. However, a consid-

erable mechanistic variability between two limiting reaction pathways is evident. One limit is a pathway with rather strong dissociative character via an eightfold-coordinated transition state of a lifetime of 10 ps. The other extreme is a pathway with nearly synchronous leaving and entering of water molecules. Since in this case the crossing point between the trajectory of the incoming and the leaving water molecules (i.e., the transition state) is displaced towards the second shell, this pathway is still most appropriately classified as a dissociative I_d interchange mechanism with weak dissociative character. A geometric explanation for the observed mechanistic exchange behaviour on $[Nd(H_2O)_9]^{3+}$ is provided in Section 5.

The 19 exchange events observed for the $[Yb(H_2O)_8]^{3+}$ aqua ion are gathered in Figure 1b. The entering and leaving of a water molecule takes place synchronously throughout with very little mechanistic variety, and therefore belongs to the group of interchange type I processes. From the experimental activation volume $\Delta V^{+} = -6\,cm^3\,mol^{-1}$ [4a] the exchange reactions for the heavy lanthanide ions of coordination number eight were classified as I_a processes. In our simulation the crossing point between the trajectory of the incoming and the leaving water molecule lay not in the middle between the first and second hydration shell, but was slightly displaced towards the inner shell (Fig. 1b), supporting an associative rather than a dissociative interchange activation mode. This point will find further corroboration in Section 5 by direct visual inspection of an exchange event on Yb^{3+} that indeed reveals a short-lived transition state of coordination number nine and of well-defined geometry.

With 50 exchanges in 1048 ps the simulation Sm represents the maximum kinetic lability of the three lanthanide ions studied. Figure 3a gives an example of the trajectories of the water molecules of the first and second hydration shell for a 100 ps interval and illustrates the equilibrium between states of eightfold and ninefold coordination. The equilibrium is maintained by a water molecule frequently exchanging between the first hydration shell and the bulk, and consequently the exchange pattern is an alternation of addition and elimination reactions. At the same time it can no longer be resolved into coupled pairs of mutually exchanging water molecules and does not fit into the classification scheme for substitution reactions with associative, dissociative and interchange-type pathways. To extract an additional feature of the reaction mechanism for simulation Sm, in Figure 4 we have superimposed those "transitory" hydration shells where an exchanging ninth water molecule is present between the first and second shell, that is, $2.6 < r_{ion-oxygen} < 3.4$ Å. For this plot we assumed square antiprismatic geometry for the eight inner water molecules and superimposed the coordination polyhedra to a maximum degree (cf. Fig. 4 in our last article[6]). The ninth water molecules have been rotated correspondingly and are shown as crosses. The surface of a square antiprism consists of two square faces and eight smaller triangular faces and, obviously, the ninth water molecule approaches the ion exclusively at one of the more easily accessible square faces. As will become evident in Section 5, this feature of the extracted configurations in Figure 4 corresponds to the addition of a water molecule to an octaaqua ion $[Yb(H_2O)_8]^{3+}$ and to the elimination of a water molecule from a nonaaqua ion $[Nd(H_2O)_9]^{3+}$.

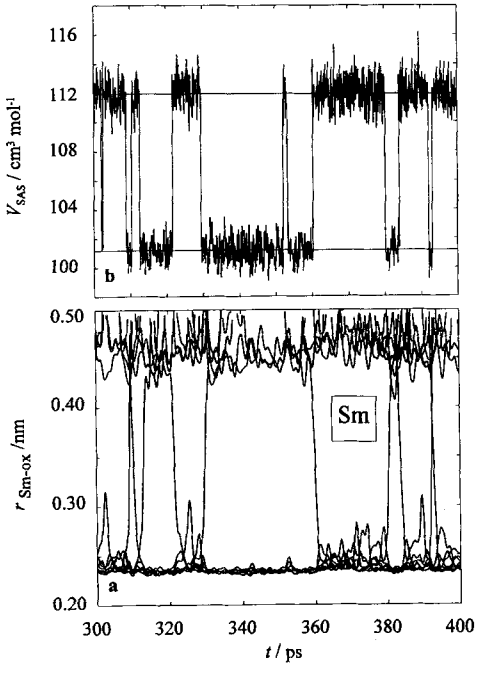

Fig. 3. a) Ion–oxygen distance for a 100 ps interval for simulation Sm (CN = 8.5) after convolution with a Gauss function (σ = 0.4 ps). The plot illustrates the equilibrium between eight- and ninefold coordination. b) The volume V_{SAS} that is enclosed by the solvent-accessible surface of the $[Sm(H_2O)_{8/9}]^{3+}$ aqua ion is shown as a function of time. The time-averaged volume is 101.2 $cm^3\,mol^{-1}$ for an octaaqua and 112.0 $cm^3\,mol^{-1}$ for a nonaaqua ion.

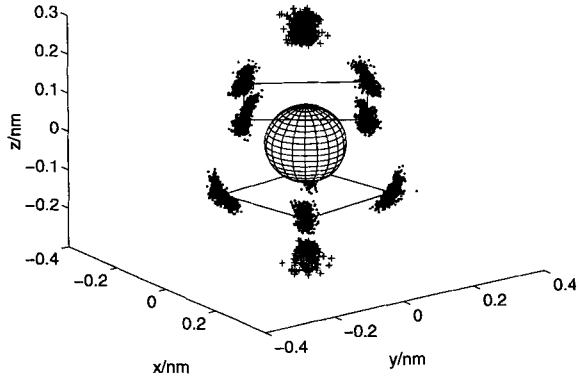

Fig. 4. "Dot plot" for those transitory hydration shells from simulation Sm where an exchanging ninth water molecule is situated between the first and second shell. For the superposition square antiprismatic geometry has been assumed for the inner octaaqua ion. The geometric centres of the point clouds are connected to guide the eye.

4. Preferential relative orientation of the two exchanging water molecules: In order to characterize the water exchange mechanism further geometrically we analysed the relative orientation between the two mutually exchanging water molecules for simulations Nd and Yb. For this purpose we calculated the angular distribution function for the angle θ formed by the incoming water molecule, the cation and the leaving water molecule. We evaluated this distribution function separately for four time intervals around the moment of exchange (t = 0.0 ps), in order to illustrate the evolution over time of the preferential relative orientation of the exchanging water molecules (Fig. 5). For simulation Nd (CN = 9) the angular distribution reveals that the two exchanging water molecules are striving for an opposing arrangement ($\cos\theta = -1$) when approaching the moment of exchange. A geometrical explanation of this behaviour will be provided in the next section.

In the case of a dissociatively activated exchange mechanism the decay of the angular correlations between the outgoing and

0947-6539/96/0203-0288 $ 15.00+.25/0 Chem. Eur. J. 1996, 2, No. 3

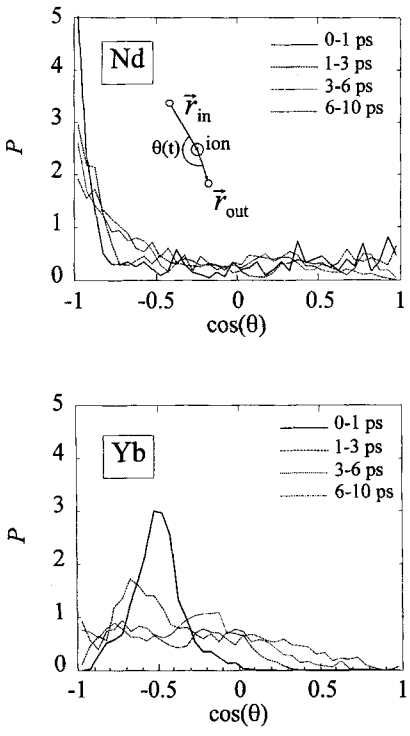

Fig. 5. Evolution in time of the angular distribution for the angle formed by the incoming water molecule, the cation and the leaving water molecule around the moment of an exchange event. Results are shown for simulation Nd (CN = 9) and simulation Yb (CN = 8).

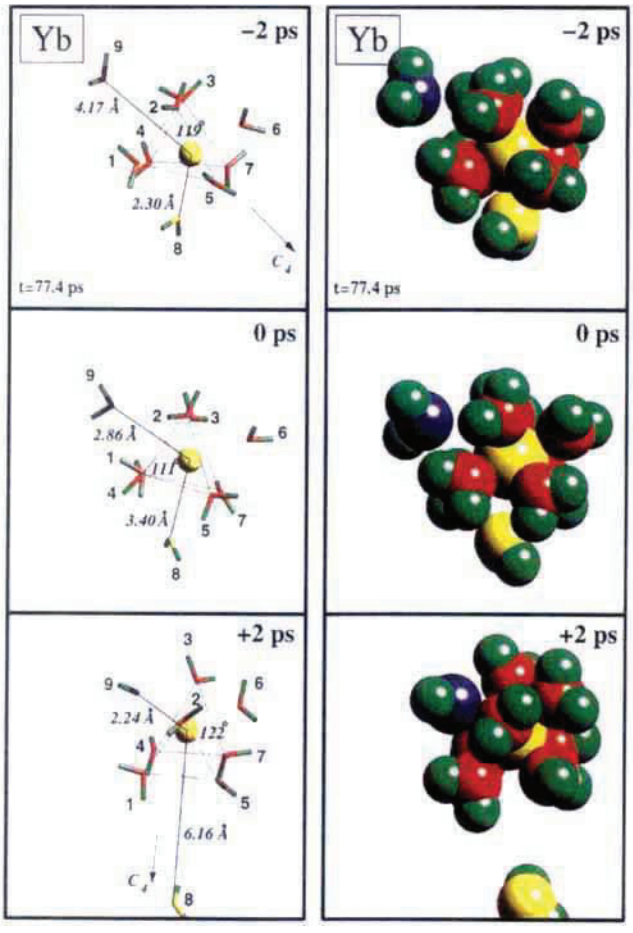

Fig. 6. Visualization of a water exchange event on a Yb^{3+} ion (CN = 8) at $t = 77.4$ ps. The incoming water molecule (9) is shown in blue, the leaving one (8) in yellow. The initial and final geometry is a square antiprism, the geometry of the transition state of coordination number nine at 0 ps is a tricapped trigonal prism.

the later incoming water molecule is caused by the decoupled reorientational diffusion of the eight-coordinated transition state and the internal rearrangement of the first hydration shell by pseudorotations of the coordination polyhedron.[6] The fact that for $[Nd(H_2O)_9]^{3+}$ a preferential relative orientation is preserved at the moment of exchange is consistent with the fact that the lifetime of the transition state (up to 11 ps) is shorter than the simulated reorientational correlation time of a Ln^{3+} aqua ion (15 ps[6]) and is at most equal to the simulated lifetime of a square antiprism between two 90° pseudorotations of the symmetry axis (11 ps[6]). It supports the classification of the exchange reaction on $[Nd(H_2O)_9]^{3+}$ as a dissociative interchange I_d mechanism that does not involve a free intermediate of coordination number eight.

For simulation Yb (CN = 8) the first hydration shell adopted the geometry of a square antiprism and water exchange was linked to a pseudorotation of the C_4 axis of the coordination polyhedron by about 65° (see Fig. 6 of ref. [6]). As Figure 5 reveals, the directions of the incoming and the leaving water molecule preferentially formed an angle of 120° ($\cos\theta = -0.5$) at the moment of exchange and therefore gave rise to another characteristic angle. In the next section we will visualize how the strong tendency of eight water molecules to form a square antiprism and of nine water molecules to form a tricapped trigonal prism when being assembled around a point charge +3 accounts for these two characteristic angles.

5. Visualization of a water exchange event for CN = 8 and 9: Figures 6 and 7 show sequences of three snapshots of the first hydration shell and of the exchanging water molecules for one exchange event on Yb^{3+} and for two exchange events on Nd^{3+}. In these figures the orientation of the outer coordinate system has been fixed during a sequence and has been chosen in such a way that the incoming and the leaving water molecules move in the plane of the paper. To guide the eye the corners of the coordination polyhedra have been connected by dashed lines and the main symmetry axis of the polyhedron is indicated. The oxygen of the incoming water molecule is rendered in blue and the oxygen of the leaving water molecule in yellow. The momentary ion–oxygen distances and oxygen-ion-oxygen angles are included for the exchanging water molecules. As has already been conjectured in Section 3, the water exchange on $[Yb(H_2O)_8]^{3+}$ proceeds via a transition state characteristic for an I_a mechanism. The sequence in Figure 6 illustrates in addition the previously mentioned oxygen-ion-oxygen angle of about 120° between the incoming water molecule (9) and the leaving water molecule (8) as well as the change in direction by about 65° of the symmetry axis C_4 of the square antiprism during an exchange event (cf. the peaks marked by a cross in Figure 6 of our last article,[6] which shows the reorientation of the C_4 axis as a function of time). The best way to pursue the exchange process is to regard the initial square antiprism at −2 ps (constituted by the square faces 1-2-3-4 and 5-6-7-8) as a dicapped trigonal prism. The vertices of the trigonal prism belonging to it have been connected in Figure 6, with water molecules 6 and 8 being the two capping ligands that stay over the rectangular faces. At −2 ps the incoming water molecule (9) attacks the initial square antiprism at one of its more easily accessible square faces. In this way it forms the missing third capping ligand for the transition state of tricapped trigonal pris-

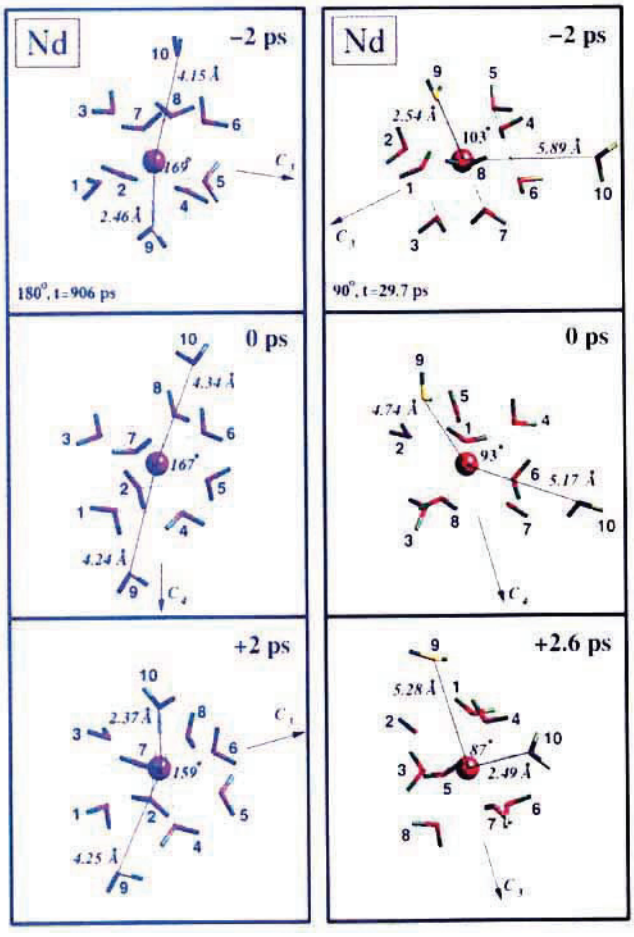

Fig. 7. Analogous plot to Figure 6 for two dissociative water exchange events on a Nd^{3+} ion (CN = 9). At t = 906 ps (left column) the transition state is a twocapped square antiprism with the leaving and incoming molecules 9 and 10 forming an angle of about 180°. At t = 29.7 ps (right column) the transition state is a capped square antiprism with the incoming water molecule (10) attacking laterally at an angle of about 90° with respect to the leaving molecule (9).

matic geometry at $t = \pm 0.0$ ps. Subsequently, the water molecule 8 is driven out of the primary hydration shell along a direction perpendicular to the square face 1-4-7-5 of the newly formed square antiprism at +2 ps, that is, in complete symmetry to the way water molecule 9 entered the first hydration shell. Interestingly, an exchange mechanism by way of the geometry of a tricapped trigonal prism has already been conjectured, from geometrical considerations and from the experimentally known activation parameters for the water exchange on the late lanthanides.[3b]

The water exchange events on $[Nd(H_2O)_9]^{3+}$ follow a dissociatively activated I_d mechanism with considerable mechanistic variability between strong and weak dissociative character (Fig. 2a). A mechanism that involves an eightfold coordinated transition state of square antiprismatic geometry nicely explains this variability as well as the preferential angular arrangement between the two exchanging water molecules (Fig. 5a). The sequence in the left-hand column of Figure 7 is a typical example. After partial dissociation of the capping water molecule 9 at −2 ps (yellow), the remaining eight water molecules adopt a geometry close to a square antiprism, with the leaving water molecule (9) staying over one of its square faces 1-4-5-2 throughout ($t = \pm 0.0$ ps). A newly entering water molecule (10, blue) approaches with the least steric hindrance by the opposite square face 3-7-6-8, in a certain sense analogously to the first step of the associative I_a mechanism on the Yb^{3+} octaaqua ion. The observed mechanistic variability reflects the lifetime distribution of the square antiprismatic transition state. It takes between roughly 0 ps (corresponding nearly to a synchronous leaving and entering of a water molecule) and approximately 10 ps (involving nearly an eightfold coordinated intermediate) before a new water molecule enters the first hydration shell. Analogously, the maximum at 180° ($\cos\theta = -1$) in the angular distribution of Figure 5a is a geometric result of the exchange by the two square faces of a square antiprism. A certain probability for angles smaller than 180° ($\cos\theta > -1$) in Figure 5a indicates that the relative orientation between the exchanging water molecules is not strictly limited to the opposing case. The right-hand column of Figure 7 shows an example where the newly entering water molecule attacks laterally in the direction of the region between the two square faces of the transient square antiprism. In both sequences presented in Figure 7 the tricapped trigonal prism is finally reestablished after complete expulsion of the molecule 9.

6. The reaction volume ΔV^0 for the coordination equilibrium between a Ln^{3+} octa- and nonaaqua ion: The activation volume $\Delta V^{\neq}$ for the water exchange reaction has been accurately determined for the eightfold coordinated heavy lanthanide ions from variable-pressure kinetic NMR experiments[4a] and should constitute another useful linkage between simulation and experiment. Before calculating, in the next section, full activation volume profiles along water exchange pathways, we will make use of the experimental and theoretical work on the reaction volume ΔV^0 for the reaction $[Ln(H_2O)_8]^{3+} + H_2O \rightleftharpoons [Ln(H_2O)_9]^{3+}$ to fine-tune a quantitative geometric definition of the effective volume of a Ln^{3+} aqua ion.

When activation volumes $\Delta V^{\neq}$ are used to distinguish between an I_a and a limiting A exchange mechanism or between an I_d and a limiting D mechanism, the activation volume $\Delta V^{\neq}_{lim}$ for the (possibly hypothetical) limiting A or limiting D mechanism must be known. $\Delta V^{\neq}_{lim}$ for the lanthanide aqua ions can be estimated from thermodynamics: the reaction volume ΔV^0 for the coordination equilibrium between an octaaqua and a nonaaqua ion $[Ln(H_2O)_8]^{3+} + H_2O \rightleftharpoons [Ln(H_2O)_9]^{3+}$ is close to the activation volume $\Delta V^{\neq}_{lim}$ for a limiting associative A mechanism on an octaaqua ion via a nonaaqua ion as the intermediate or, likewise, close to the negative activation volume for a limiting dissociative D mechanism on a nonaaqua ion via an octaaqua ion.

The reaction volume ΔV^0 for the coordination equilibrium in question can be estimated from geometric considerations. An example is Swaddle's semiempirical model for the partial molar volume of metal aqua ions at infinite dilution.[16] In this model the partial molar volume $\bar{V}^0_{abs}$ is calculated as the effective volume of the aqua ion $[M(H_2O)_n]^{z+}$ minus the molar volume of pure water ($n \times 18.07\ cm^3\,mol^{-1}$) and minus the volume contraction due to the electrostriction of the solvent beyond the first coordination sphere of the ion [Eq. (2), V in $cm^3\,mol^{-1}$, r and Δr in pm]. The aqua ion is assumed to be spherical and

$$\begin{aligned} \bar{V}^0_{abs} &= V_{aqua\ ion} - V_{molar} - V_{electrostriction} \\ &= 2.523 \times 10^{-6}(r+\Delta r)^3 - 18.07n - 417.5z^2/(r+\Delta r) \end{aligned} \quad (2)$$

its effective volume is estimated from its effective radius $(r + \Delta r)$, where r is the ionic radius and Δr is the effective diameter of a water molecule that allows for deviations from ideal close-packing in the first shell and for imperfect interfacing with the bulk solvent. With coordination number sensitive ionic radii r from Shannon[17] and by fitting Δr to some well-characterized aqua ions, Swaddle's model can successfully predict the partial

0947-6539/96/0203-0290 $ 15.00+.25/0 Chem. Eur. J. 1996, 2, No. 3

molar volumes of a variety of aqua ions of different ionic charge and coordination number. In particular the model can reproduce the observed partial molar volumes for lanthanide(III) octa- and nonaaqua ions[18] and can supply separate values for those ions in the middle of the lanthanide series where both types of coordination coexist and only an average value can be measured. The difference between the partial molar volumes of the two types of coordinated ions, the reaction volume ΔV^0 for the coordination equilibrium, is practically a constant along the lanthanide series (varying from $-12.5\ cm^3 mol^{-1}$ for La^{3+} to $-13.1\ cm^3 mol^{-1}$ for Lu^{3+}). Experimentally, a value for ΔV^0 of $-10.9\ cm^3 mol^{-1}$ has been derived from the pressure dependence of the coordination equilibrium between $[Ce(H_2O)_8]^{3+}$ and $[Ce(H_2O)_9]^{3+}$.[19] Swaddle's model gives absolute values for the partial molar volume of the lanthanide octaaqua ions that are too large by nearly $2\ cm^3 mol^{-1}$ compared with the experimental values (see Fig. 2 of ref. [16b]). Therefore, the calculated absolute reaction volumes $|\Delta V^0|$ should naturally be overestimated by the same amount.

From our MD simulations the reaction volume ΔV^0 could be obtained in two ways. The first and rather computationally intensive possibility was a thermodynamic approach by means of $K = K_0 \exp(-P\Delta V^0/RT)$ by studying the pressure (density) dependence of the equilibrium constant K for the coordination equilibrium between the octaaqua and nonaaqua ion directly. For a reliable estimation of ΔV^0 we performed two additional NVT simulations for Sm^{3+} in aqueous solution at overall densities of $\rho = 0.90$ and $1.10\ g cm^{-3}$, in order to supplement our simulation at ambient pressure.[2] We assumed that the potential energy function model was still valid for densities other than $1.0\ g cm^{-3}$ and applied the same simulation scenario as in ref. [2] for a simulation time of 512 ps. Figure 8 shows the result-

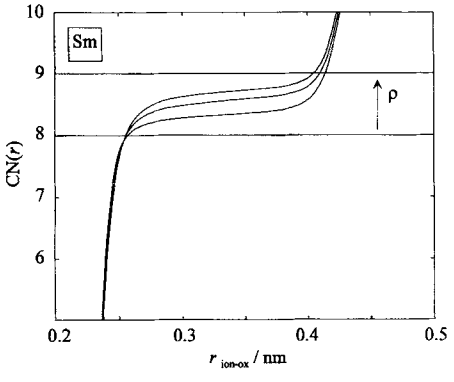

Fig. 8. Effect of the overall density ρ on the running coordination number of a Sm^{3+} ion in aqueous solution. From bottom to top: $\rho = 0.900, 1.013, 1.100\ g cm^{-3}$.

ing running coordination number of Sm^{3+}, and Figure 9 displays the distribution of the number of water molecules in different ion–oxygen distance ranges. In Table 1, densities have been converted into pressure values by the experimental compressibility of pure water ($\kappa = 4.58 \times 10^{-5}\ bar^{-1}$[20]), and the equilibrium constant K has been calculated from the percentage of the eight- and ninefold coordinated Sm^{3+} aqua ions (Fig. 9, hatched bars). From the slope of a plot of $\ln K(p)$ (Fig. 10) the reaction volume ΔV^0 emerges as $-8.3\ cm^3 mol^{-1}$.

The success of Swaddle's model motivates an alternative estimation of ΔV^0 that is purely geometric. This approach makes use of the fact that the analysis of a MD simulation of one ion in solution distinguishes between configurations with either the octaaqua or the nonaaqua ion present. The reaction volume

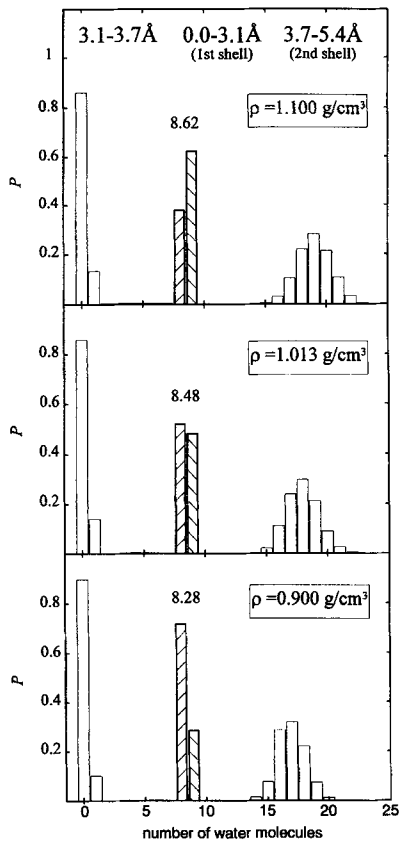

Fig. 9. Distribution of the number of water molecules in three distance ranges around the Sm^{3+} ion at three different overall densities. In each of the three distance ranges the sum of the mole fractions p equals 1. The inserted numbers are the mean numbers of water molecules in each distance range.

Table 1. Pressure effect on the equilibrium constant K for the coordination equilibrium $[Sm(H_2O)_8]^{3+} + H_2O \rightleftharpoons [Sm(H_2O)_9]^{3+}$. p_8 and p_9 are the mole fractions of an eight- and a ninefold coordinated Sm^{3+} aqua ion from Figure 9.

density, $g cm^{-3}$	0.900	1.013	1.100
Δp, bar	−2440	0	1880
p_9	0.283	0.481	0.622
p_8	0.717	0.519	0.378
$K = p_9/p_8$	0.395	0.926	1.646

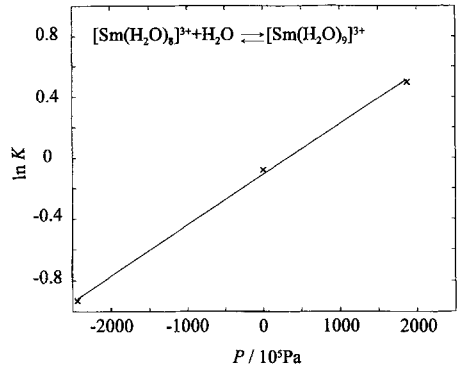

Fig. 10. Logarithm of the equilibrium constant K as a function of pressure for the coordination equilibrium $[Sm(H_2O)_8]^{3+} + H_2O \rightleftharpoons [Sm(H_2O)_9]^{3+}$.

ΔV^0 is then the difference V_{tot} (CN = 9) − V_{tot} (CN = 8) between the mean total volume of the system for a ninefold- and an eightfold-coordinated ion. Unfortunately, as the volume is a widely fluctuating quantity in MD simulations, the effect

of the change in the coordination number on the overall density will hardly be detectable. Nevertheless, as in Swaddle's model, it can be assumed firstly that the volume effect on the bulk consists only in the removal of a water molecule ($-V_{H_2O} = -18.07\ cm^3 mol^{-1}$) and secondly that the structural effects of a change in the coordination number are confined to a certain region around the cation. In this way the key difficulty is reduced to finding a reasonable quantitative definition of the effective volume of an aqua ion $[Ln(H_2O)_n]^{3+}$.

We abstained from treating the aqua ion as a hard sphere as in Swaddle's model and instead evaluated its volume as that which is enclosed by its solvent-accessible Connolly surface.[21] Especially for bioorganic applications the solvent-accessible surface is widely used to interpret and correlate thermodynamic quantities and, in our case, it offers the additional advantage of giving access to the full volume profile along a water exchange pathway, which will be evaluated in the next section. Connolly surfaces were computed from the water oxygens in the first shell by means of the Cerius^2 program[22] and a probe radius of 1.40 Å was employed. The success of Swaddle's model and its superiority over former models is, among other things, based on the use of an *effective* density of water in the first hydration shell that has been fitted to experimental partial molar volumes of aqua ions. Analogously, we adjusted the hard-sphere radius of a water oxygen in the first shell, the key parameter for the construction of the Connolly surface, with reference to the effective volumes of lanthanide aqua ions $[Ln(H_2O)_n]^{3+}$ from Swaddle's model. In Table 2 the effective volumes from Swaddle's model and from our simulations (applying an optimized water-oxygen hard-sphere radius of 1.72 Å) are compared. In Figure 3b the Connolly volume V_{SAS} enclosed by the surface of the first hydration shell of the Sm^{3+} aqua ion is given as a function of time. With V_{SAS} (CN = 9) = 112.0 $cm^3 mol^{-1}$ and V_{SAS} (CN = 8) = 101.2 $cm^3 mol^{-1}$ we obtained $\Delta V^0 = (112.0 - 101.2 - 18.07)\ cm^3 mol^{-1} = -7.2\ cm^3 mol^{-1}$ (Table 2).

In conclusion, we have shown that the simulated thermodynamic value for ΔV^0 can be consistently reproduced from a geometric approach that uses calibrated Connolly surfaces. It has to be conceded that both calculated values are too positive by 3–4 $cm^3 mol^{-1}$ compared with an experimental value close to $-10.9\ cm^3 mol^{-1}$.[19] Nevertheless, taking into account that even a change of 0.01 Å in the mean radius of the aqua ion corresponds to a change of 1 $cm^3 mol^{-1}$ in the volume,[16] this deviation is still acceptable. In the next section we will use Connolly surfaces to calculate the profile of the relative volume change during a water exchange event.

7. The volume profile $\Delta V^{\neq}(t)$ for water exchange: The recent calculation of $\Delta V^{\neq}$ for the exchange of coordinated water from a quantum-mechanical study of metal-ion aqua clusters has caused some controversy and as a result some assumptions concerning the mechanistic interpretation of experimental activation volumes have been questioned.[23] It has been suggested that the electrostriction of the incoming water molecule or the change in the bond distances of the nonparticipating ligands might aggravate the difficulties of reliable interpretation of small activation volumes and necessitate additional results from other methods. Whereas a quantum-mechanical study cannot explicitly take into account the statistical nature of the surrounding bulk water and assumes ground and transition states of ideal geometry at 0 K, a simulation approach to $\Delta V^{\neq}$ avoids these limitations and at the same time provides more insight into the mechanistic variability of the full exchange pathway.

The mean activation volume $\Delta V^{\neq}$ for the water exchange can be derived from MD simulations by $k_{ex} = k_{ex,0} \times \exp(-P\Delta V^{\neq}/RT)$ by studying the pressure dependence of the water exchange rates k_{ex}. This thermodynamic approach is hampered by its considerable computational demand: on the typical timescale of MD simulations (1 ns), water exchanges on lanthanide ions are still rare events and, as test calculations revealed, even for a simulation time of 1 ns the statistical uncertainty in the simulated exchange rates was close to the effect of pressure on the rates. Consequently, a reliable evaluation of the activation volume would necessitate several long-time simulations of at least 1 ns for different pressures.

As a more economical expedient we instead estimated geometrically the relative volume change along the detected water exchange reaction pathways in our constant pressure simulations. For the calculation of the detailed volume profile we assumed, as in the previous section, that density changes were confined to the first hydration shell, and defined the relevant region by its Connolly surface. An example of the surface enclosing both the aqua ion and the exchanging water molecule is given in Figure 11. The mean volume profiles $\Delta V^{\neq}(t)$ from the

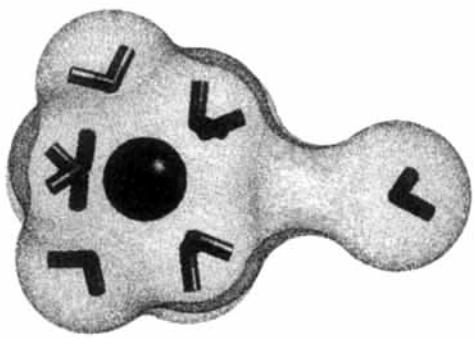

Fig. 11. Example of the solvent-accessible surface enclosing the $[Yb(H_2O)_8]^{3+}$ aqua ion and an exchanging water molecule. The graphic was produced with the CERIUS^2 package [22].

water exchanges on a $[Nd(H_2O)_9]^{3+}$ and a $[Yb(H_2O)_8]^{3+}$ aqua ion are shown in Figures 12a and 13a for a 10 ps interval around the moment of exchange. Volume changes are given with respect to the mean volume of an aqua ion in equilibrium plus one isolated water molecule, that is, $V([Nd(H_2O)_9]^{3+} + H_2O) = 129.0\ cm^3 mol^{-1}$ and $V([Yb(H_2O)_8]^{3+} + H_2O) = 109.7\ cm^3 mol^{-1}$. Furthermore, in Figures 12b and 13b symmetry in time with respect to the moment of exchange has been

Table 2. Comparison of characteristic volumes for lanthanide aqua ions from Swaddle's semiempirical model [16] and from the MD simulation with Connolly surfaces that enclose the first hydration shells (volume in $cm^3 mol^{-1}$). ΔV^0 is the resulting reaction volume for the coordination equilibrium on a Sm^{3+} aqua ion.

	Swaddle [16]		MD simulation			
	$[Nd(H_2O)_9]^{3+}$	$[Yb(H_2O)_8]^{3+}$	$[Nd(H_2O)_9]^{3+}$	$[Sm(H_2O)_9]^{3+}$	$[Sm(H_2O)_8]^{3+}$	$[Yb(H_2O)_8]^{3+}$
V_{eff} [a]	112.9	96.7	114.97	112.00	101.17	96.02
ΔV^0 [b]				−7.24		

[a] V_{eff} = Effective volume of the aqua ion. [b] $\Delta V^0 = V(CN = 9) - V(CN = 8) - 18.07$ for $[Sm(H_2O)_8] + H_2O \rightleftharpoons [Sm(H_2O)_9]$

0947-6539/96/0203-0292 $ 15.00+.25/0 Chem. Eur. J. 1996, 2, No. 3

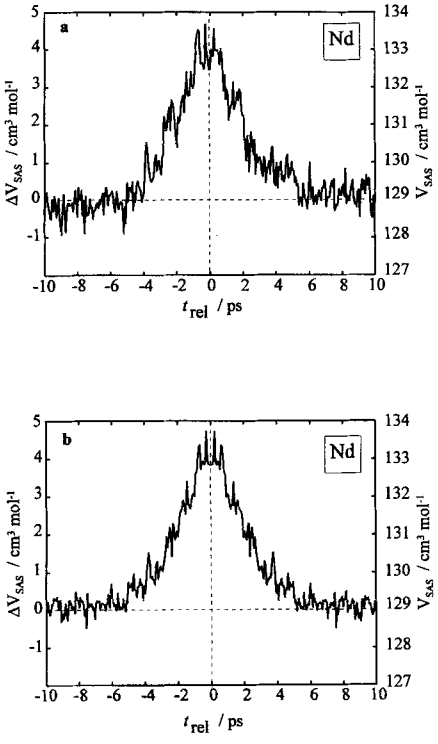

Fig. 12. a) Mean activation volume profile $\Delta V_{SAS}(t)$ from the water exchanges on Nd^{3+} (CN = 9). The volume is that enclosed by the solvent-accessible surface of the ten water molecules participating in the exchange process. b) Symmetrized volume profile after averaging the positive and the negative halves of the profile in a).

imposed, by averaging the negative and the positive halves from Figures 12a and 13a, respectively. For $[Nd(H_2O)_9]^{3+}$ (Fig. 12) the dissociation of a water molecule from the primary hydration shell corresponds to an increase in volume by about $+4.5\ cm^3\,mol^{-1}$. This value is significantly smaller than the activation volume of $7-8\ cm^3\,mol^{-1}$ for a limiting dissociative mechanism that was estimated in the previous paragraph, and corroborates the assignment of the mean exchange mechanism as I_d. The picture that emerges from the volume profile for the water exchange on $[Yb(H_2O)_8]^{3+}$ (Fig. 13) is as follows: the moment when a water molecule from the second hydration shell enters the region between the first and second sphere (≈ 2 ps before the moment of exchange, Fig. 1b) corresponds to a first transition state of slightly increased volume. This feature of the volume profile indicates that the square antiprismatic octaaqua ion prepares itself geometrically for the reception of a ninth water molecule before compacting again to a second transition state, that is, a more symmetric and less voluminous nonaaqua ion of tricapped trigonal prismatic geometry at $t = 0$ ps. The fact that the volume of the transition state at $t = 0$ ps is only slightly smaller than the volume of the octaaqua ion plus the volume of an isolated water molecule results in a slightly negative mean activation volume and disagreed with the experimental activation volume of $-6\ cm^3\,mol^{-1}$ for octaaqua ions.[4b] This deficiency is probably due to the fact that the two exchanging water molecules are not penetrating deeply enough into the first hydration shell (Fig. 6) and reveals an insufficiency of the applied potential energy function, which cannot, however, be easily remedied. From ab initio cluster calculations of the water exchange reaction of the Be^{2+} aqua ion in vacuo, the calculated activation volume $\Delta V^{\neq}$ was found to be approximately equal to 0, compared with the experimental value of $-13.6\ cm^3\,mol^{-1}$; the discrepancy has been attributed to the incomplete description of the second coordination shell.[24] In our case it is likewise conceivable that the neglect of volume effects in the second hydration sphere contributes to the discrepancy with the experimental value.

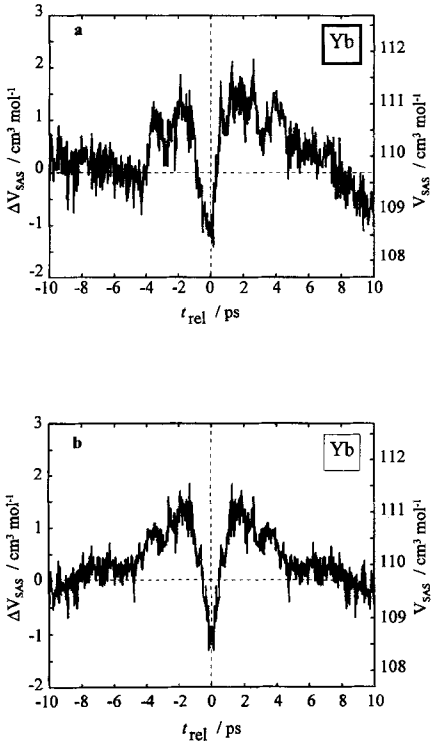

Fig. 13. a) Mean activation volume profile $\Delta V_{SAS}(t)$ from the water exchanges on Yb^{3+} (CN = 8). The volume is that enclosed by the solvent-accessible surface of the nine water molecules participating in the exchange process. b) Symmetrized volume profile.

Although the quantitative agreement with experimental reaction and activation volumes is not perfect, some interesting qualitative points from the simulation approach are worthy of note. Firstly, properties linked to the volume of aqua ions are rarely considered in simulation studies, but may be a useful criterion for the rigorous testing of the degree of reality of a simulation. Secondly, the full volume profile, which is not accessible by experimental methods or quantum mechanical calculations, might contain more than one transition state/intermediate and might be poorly represented by an average activation volume. This may hamper mechanistic interpretations of an experimental mean $\Delta V^{\neq}$ value, especially for small activation volumes; in our case, the simulated volume profile for the exchange on $[Yb(H_2O)_8]^{3+}$ indicated a mean activation volume close to zero, whereas direct visual inspection revealed the characteristics of an associative interchange I_a mechanism (Fig. 6). Finally, in the quantum mechanical study of ref. [23] aqua ions and water molecules were assumed to be hard spheres for the calculation of the volume of metal-ion aqua clusters and of activation volumes. Hence, without careful calibration of the effective hard-sphere radius, a geometric value for the activation volume might deviate from the true thermodynamic value.

Summary and Outlook

MD simulations were used to provide insight into geometric and mechanistic aspects of the water exchange reaction on Ln^{3+} aqua ions that cannot or can only indirectly be inferred from experiment.

Along the series of the lanthanide ions a shift from predominant ninefold to predominant eightfold coordination is accompanied by a changeover concerning the water exchange mechanism. The water exchange on $[Nd(H_2O)_9]^{3+}$ can be assigned a dissociative interchange I_d mechanism from the mean activation volume $\Delta V^{\neq}$, which was clearly smaller than the estimated value $\Delta V^{\neq}_{lim}$ for a limiting dissociative D mechanism. Direct inspection of the exchange reaction pathways revealed considerable mechanistic variability between strong and weak dissociative character. This variability reflects the lifetime of the square antiprismatic transition state of a coordination number near eight. A limiting dissociative D mechanism involving a free eightfold coordinated state could be further excluded since the lifetime of the transition state was shorter than the reorientational correlation time of the complex and the two exchanging water molecules preserved a preferential opposing orientation. For $[Yb(H_2O)_8]^{3+}$ the exchange reaction followed an interchange-type scheme involving a slightly negative mean activation volume. Direct visual inspection of the reaction pathways revealed the characteristics of an I_a mechanism: the exchange of two water molecules took place synchronously via a transition state geometry close to a tricapped trigonal prismatic coordination polyhedron that was slightly more compact than the separate entities, that is, one octaaqua ion plus one isolated water molecule. The well-defined transition state geometry imposed a strong preferential relative orientation between the exchanging water molecules. For Sm^{3+}, a frequently exchanging water molecule maintains the coordination equilibrium between eight- and ninefold coordination. The alternating of elimination and addition events could not be resolved into pairs of mutually exchanging water molecules and the concept of D, I or A processes for substitution processes does not apply. For all lanthanide ions the details of the observed mechanisms and of the involved transition states could be geometrically rationalized by the strong tendency of eight water molecules to form a square antiprism and of nine water molecules to form a tricapped trigonal prism around the cation.

From a broader perspective one might ask whether the observed dependence of the solvent exchange mechanism on the coordination number is typical only for aqueous solutions or if it is more generally valid for polar solvents. To clarify this question, *N*,*N*-dimethylformamide (DMF) suggests itself as another solvent for further simulations. DMF, like water, is a "hard" oxygen-donor solvent with a high dipole moment, and the Ln^{3+}–DMF interaction should likewise be well represented by a point charge model. Furthermore, a simulation series with DMF could be used to test whether the approaches that have been developed for describing solvent polarization and for the analysis of aqueous solutions and that are specially adapted to the high positive charge of the cation are extendable to other solvents and are therefore of broader significance.

Acknowledgements: This work was supported by the Swiss National Science Foundation (Grant No 20-39483.93) and the Swiss OFES as part of the European COST D 3 action.

Received: August 17, 1995 [F190]

[1] S. Galera, J. M. Lluch, A. Oliva, J. Bertrán, F. Foglia, L. Helm, A. E. Merbach, *New J. Chem.* **1993**, *17*, 773–779.
[2] Th. Kowall, F. Foglia, L. Helm, A. E. Merbach, *J. Am. Chem. Soc.* **1995**, *117*, 3790–3799.
[3] a) C. Cossy, A. C. Barnes, J. E. Enderby, A. E. Merbach, *J. Chem. Phys.* **1989**, *90*, 3254–3260; b) L. Helm, A. E. Merbach, *Eur. J. Solid State Inorg. Chem.* **1991**, *28*, 245–250; c) C. Cossy, L. Helm, D. H. Powell, A. E. Merbach, *New J. Chem.* **1995**, *19*, 27–35.
[4] a) C. Cossy, L. Helm, A. E. Merbach, *Inorg. Chem.* **1988**, *28*, 2699–2703; b) K. Micskei, D. H. Powell, L. Helm, E. Brücher, A. E. Merbach, *Magn. Reson. Chem.* **1993**, *31*, 1011–1020; c) D. H. Powell, A. E. Merbach, *ibid.* **1994**, *32*, 739–745.
[5] For a summary of the imperfections of our theoretical model, see footnote 2 of ref. [6].
[6] Th. Kowall, F. Foglia, L. Helm, A. E. Merbach, *J. Phys. Chem.* **1995**, *99*, 13078–13087.
[7] J. W. Akitt, A. E. Merbach, *NMR Basic Principles and Progress, Vol. 24* (Eds.: P. Diehl, E. Fluck, R. Kosfeld), Springer, Berlin/Heidelberg, **1990**, p. 189.
[8] R. van Eldik, A. E. Merbach, *Comments Inorg. Chem.* **1992**, *12*, 341–378.
[9] C. H. Langford, H. B. Gray, *Ligand Substitution Processes*, W. A. Benjamin, New York, **1965**.
[10] S. Hengrasmee, M. M. Probst, *Z. Naturforsch.* **1991**, *46a*, 117–121.
[11] R. W. Impey, P. A. Madden, I. R. McDonald, *J. Phys. Chem.* **1983**, *87*, 5071–5083.
[12] a) R. A. Plane, H. Taube, *J. Chem. Phys.* **1952**, *56*, 33; b) J. P. Hunt, H. Taube, *ibid.* **1951**, *19*, 602.
[13] a) R. Caminiti, G. Licheri, G. Piccaluga, G. Pinna, *J. Phys. Chem.* **1976**, *65*, 3134–3138; b) R. Caminiti, G. Licheri, G. Piccaluga, G. Pinna, *J. Chem. Phys.* **1978**, *69*, 1–4; c) R. D. Broadbent, G. W. Neilson, M. Sandstrøm, *J. Phys. Condens. Matter* **1992**, *4*, 639-648; d) M. C. Read, M. Sandstrøm, *Acta Chem. Scand.* **1992**, *46*, 1177–1182.
[14] a) W. L. Earl, doctoral thesis, University of California, **1975**; b) A. Bleuzen, F. Foglia, L. Helm, A. E. Merbach, unpublished results.
[15] a) P.-Å. Bergström, J. Lindgren, M. Read, M. Sandström, *J. Phys. Chem.* **1991**, *95*, 7650–7655; b) P.-Å. Bergström, J. Lindgren, *Inorg. Chem.* **1992**, *31*, 1529–1533.
[16] a) T. W. Swaddle, *Adv. Inorg. Bioinorg. Mechanisms* **1983**, *2*, 95–135; b) T. W. Swaddle, M. K. S. Mak, *Can. J. Chem.* **1983**, *61*, 473–480.
[17] R. D. Shannon, *Acta Crystallogr. Sect. A* **1976**, *32*, 751.
[18] F. H. Spedding, M. J. Pikal, B. O. Ayres, *J. Phys. Chem.* **1966**, *70*, 2440–2449.
[19] G. Laurenczy, A. E. Merbach, *Helv. Chim. Acta* **1988**, *71*, 1971–1973.
[20] N. S. Isaacs, *Liquid Phase High Pressure Chemistry*, Wiley, Chichester/New York/Brisbane/Toronto, **1981**, p. 80.
[21] M. L. Connolly, *Science* **1983**, *221*, 709–713.
[22] Cerius² v. 1.1 is available from Molecular Simulations, Cambridge, UK.
[23] R. Åkesson, L. G. M. Pettersson, M. Sandström, U. Wahlgren, *J. Am. Chem. Soc.* **1994**, *116*, 8705–8713.
[24] M. A. Lee, N. W. Winter, W. H. Casey, *J. Phys. Chem.* **1994**, *98*, 8641–8647.

0947-6539/96/0203-0294 $ 15.00+.25/0